Prediction of an Excitonic Ground State in InAs/InSb Quantum Dots

Lixin He, Gabriel Bester, and Alex Zunger
National Renewable Energy Laboratory, Golden, Colorado 80401, USA
(Received 6 May 2004; published 3 January 2005)

Using atomistic pseudopotential and configuration-interaction many-body calculations, we predict an excitonic ground state in the InAs/InSb quantum-dot system. For large dots, the conduction band minimum of the InAs dot lies below the valence band maximum of the InSb matrix. Due to quantum confinement, at a critical size calculated here for various shapes, the gap E_g between InAs conduction states and InSb valence states vanishes. Strong electron-hole correlation effects are induced by the spatial proximity of the electron and hole wave functions, and by the lack of strong (exciton unbinding) screening, afforded by the existence of discrete 0D confined energy levels. These correlation effects overcome E_g, leading to the formation of a biexcitonic ground state (two electrons in InAs and two holes in InSb) being energetically more favorable (by $\sim$15 meV) than the dot without excitons.

DOI: 10.1103/PhysRevLett.94.016801 PACS numbers: 73.21.La, 71.35.Lk, 73.22.–f

The formation of excitons in semiconductors and insulators usually requires energy, e.g., photons, for one has to excite carriers across the single-particle band gap E_g. There is a special interest, however, in the possibility of forming excitons exothermically, i.e., an ''excitonic ground state'' as envisioned by Mott [1] and Keldysh *et al.* [2]. Indeed, the electron-hole system exhibits a rich range of phases [3,4] as a function of the carrier density and effective-mass ratio m_e/m_h, including various excitonic insulating states such as molecular solid, exciton liquid, Mott insulator, and also various metallic phases. The excitonic ground state is of fundamental interest in itself because excitons can be a better alternative to atoms for studying Bose-Einstein condensation [5,6] on account of the lighter excitonic mass, thus higher condensation temperature. It is natural to search for excitonic ground states in systems where E_g is small, yet the screening is weak enough so as to prevent unbinding of the exciton. The search in *bulk solids* [7] has thus focused on *indirect* gap semiconductors and semimetals to reduce screening, but excitonic ground states have not been conclusively observed so far in such systems. Ground state excitons were also searched in *nanostructures*, specifically in spatially indirect quantum wells [8,9], where electrons and holes are confined in different spatial regions. In ''type II'' systems such as GaInAs/InP or CdTe/CdSe, electrons are localized in the well, whereas holes are localized on the barrier, so screening is weak, but E_g is finite. In contrast, in ''type III'' heterostructures such as [10] InAs/GaSb, the conduction band minium (CBM) of the InAs well is lower than the valence band maximum (VBM) of the GaSb barrier, so at certain well thickness one can have $E_g \rightarrow 0$ [10], as well as separation of electrons from holes. Thus, at this thickness, one could expect an excitonic ground state if the electron-hole correlation energy will be large enough to stabilize the complex. Recent experiments [11] show evidence for an existing excitonic ground state in type III InAs/$Al_xGa_{1-x}Sb$ quantum-well superlattices; however, the binding energy was small (estimated at $\sim$3–4 meV) and strong magnetic fields are needed to stabilize the system. This is because in a 2D periodic well or superlattice, extended states exist in the in-pane direction leading to rather weak excitonic binding.

The advantage of a type III system can, however, be utilized without the disadvantage of 2D periodicity underlying a quantum well, if one considers a type III *0D quantum dot* (QD). The well known InAs/$Al_xGa_{1-x}Sb$ epitaxial system [11] is inappropriate here, since it is lattice matched, so dots will not form in a strain-induced Stranski-Krastanov (SK) growth [12]. We propose here a new dot/matrix system, InAs/InSb, which has a type III band alignment [13], and a lattice mismatch, and is hence amenable to epitaxial SK growth. Using an empirical pseudopotential approach [14], we find that as the dot size is reduced, electron levels localized on InAs move up in energy, whereas hole states, localized at the interface, initially above the electron levels, move down in energy. The system reaches a degeneracy $E_g \sim 0$ of electron and hole single-particle levels at a critical size, predicted here for different dot shapes. As a result of the 0D confinement of both electrons and holes, there is but a small number of fully discrete bound states, so screening is limited, helping the binding of the particles. Furthermore, the strain in the lens-shaped or spherical dots localized the holes at the interface near the dot, thus offering proximity which is conducive to electron-hole binding. Using many-body configuration interaction (CI), we find that consequently, at the critical size, the exciton is bound by as much as $\sim$15 meV $\gg E_g$, thus forming an excitonic ground state. Our study characterizes theoretically the properties of the excitonic ground state in this system, offering experimentally testable predictions.

Identifying the material system.—The customary way of selecting a *strained* dot/matrix system [12] is to require that the dot material has a smaller gap than the matrix material (e.g., InAs/GaAs or CdSe/ZnSe) so that all car-

riers can be confined inside the dot. In conventional semiconductors [15] the requirement $E_g^{\text{dot}} < E_g^{\text{matrix}}$ implies $a^{\text{dot}} > a^{\text{matrix}}$, where a is the bulk lattice constant, leading to compressive strain. Here, however, we seek $E_g \to 0$ with spatially separated, yet confined carriers, so we look for a system where the CBM of the dot material is *below* the VBM of the matrix material. This could be met when the dot material has a *larger* band gap (thus, a smaller lattice constant) than the matrix material, leading to *tensile* strain. SK growth under tensile strain was demonstrated before for PbTe/PbSe [16], but not for InAs/InSb, which we feel is potentially a very interesting challenge. The InAs/InSb system [10] has a lattice mismatch of $\sim 7\%$, and the CBM of InAs is below the VBM of InSb by 0.17 eV for the unstrained system. This guarantees that the electrons will be confined on InAs, and holes on InSb. We will see below that one can further chose a strained dot *shape* that will bring the holes to the interface, thus providing proximity, yet spatial separation of electrons and holes.

Strain and confinement.—We have tested various dot shapes and sizes. Here we show three lens-shaped InAs dots of base/height = 104/26, 143/36, and 156/39 Å labeled as D1, D2, and D3, respectively, as well as spherical dots, all embedded in an InSb matrix. The supercell that includes the dot and the matrix contains up to about 6×10^5 atoms. The strain is relaxed by minimizing the strain energy with respect to the displacement of all atoms, representing the energy as a sum of bond-bending and bond-stretching force constants (the valence force field method (VFF) [17]). The VFF and pseudopotential parameters are taken from Ref. [13]. Denoting by $\epsilon_{\alpha\beta}$, the $\alpha\beta$ component of the strain tensor, Fig. 1(a) shows the strain profile along the [001] direction across the dot D2, demonstrating that the isotropic strain $I = \epsilon_{xx} + \epsilon_{yy} + \epsilon_{zz}$ is positive (tensile), almost a constant inside the dots and decays to zero very rapidly in the barrier, whereas the biaxial component $B = [(\epsilon_{xx} - \epsilon_{yy})^2 + (\epsilon_{yy} - \epsilon_{zz})^2 + (\epsilon_{zz} - \epsilon_{xx})^2]^{1/2}$ is nonzero and nonconstant inside the dot, but decays slowly to zero outside. To observe how this strain modifies the electronic properties, we show in Fig. 1(b) the strain-modified confining potentials obtained by inserting the strain of Fig. 1(a) into the Pikus-Bir equations [18]. The isotropic strain lowers both the CBM and the VBM of InAs, but the lowering of CBM is greater, leading to a large reduction of the gap from the unstrained bulk value of 0.42 to 0.01 eV. Very importantly, because of the curved shape of the strained dot leading to a large biaxial strain at the interface, the heavy-hole potential has a maximum at the InAs/InSb *interface*. We thus expect (and find below) that hole states will localize at the interface, rather than be extended throughout the barrier. This will enhance electron-hole binding.

Method of calculation.—We relax the atomic position, $\{\mathbf{R}_{i,\alpha}\}$ via the VFF method and construct the total pseudopotential of the system $V(\mathbf{r})$ by superposing the local,

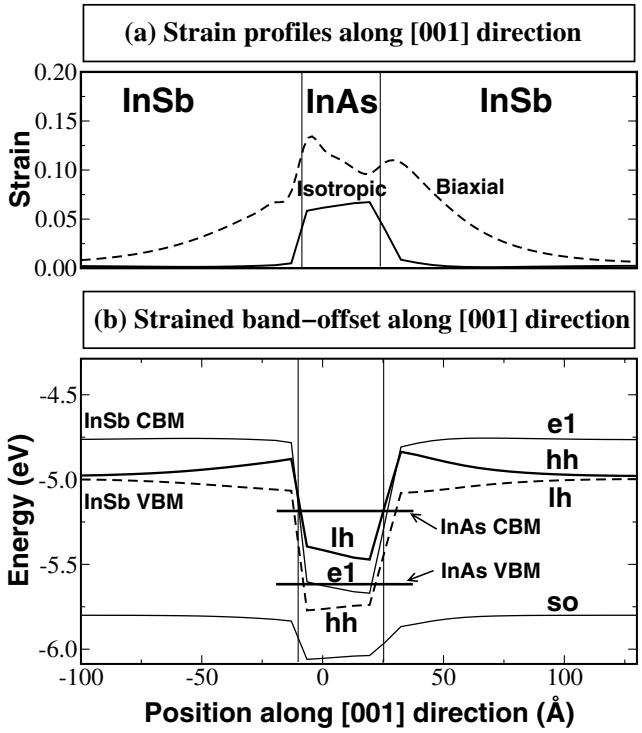

FIG. 1. (a) The isotropic and biaxial strain profiles along the [001] direction; (b) Strain-modified band offset along the [001] direction calculated from the Pikus-Bir model. The *unstrained* InAs and InSb band edges are also indicated as "InAs CBM," "InAs VBM," "InSb CBM," and "InSb VBM". Here, $e1$, hh, 1h, and s.o. denote the band characters of the confining potentials. Note the reversal of the hh/lh characters inside vs outside the QDs.

screened atomic pseudopotential $v_\alpha(\mathbf{r})$ of all (dot + matrix) atoms and the nonlocal spin-orbit potentials $V_{\text{s.o.}}$: $V(\mathbf{r}) = V_{\text{s.o.}} + \sum_{i,\alpha} v_\alpha(\mathbf{r} - \mathbf{R}_{i,\alpha})$. We do not include the piezo effect, since we find it is small in this case. We use the linear combination of bulk band (LCBB) method [19], where the Hamiltonian $-1/2\nabla^2 + V(\mathbf{r})$ is diagonalized in a basis $\{\phi_{n,\epsilon,\lambda}(\mathbf{k})\}$ of Bloch orbitals of band index n and wave vector $\mathbf{k}$ of material λ(= InAs, InSb, and GaAs), strained uniformly to strain ϵ. This LCBB approach [19] produces accurate results for many nanostructures [20], and greatly surpasses in accuracy the $\mathbf{k} \cdot \mathbf{p}$ method, which limits the basis to $n = \text{VBM} + \text{CBM}$ at $\mathbf{k} = 0$ only. Many-body effects are included via the CI method [21] by expanding the total wave function in Slater determinants for single and biexcitons formed from all of the confined single-particle electron and hole states. The Coulomb and exchange integrals are computed numerically from the pseudopotential single-particle states, using the microscopic position-dependent dielectric constant [21]. Our CI approach is very similar to the Bethe-Salpeter equations [22], except that in the latter case all the exchange integrals are unscreened, whereas since the

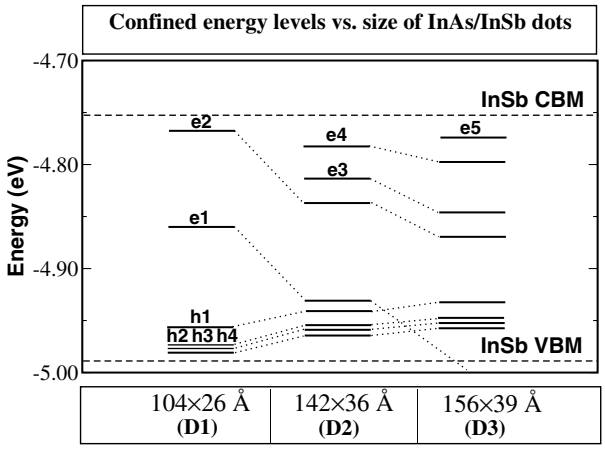

FIG. 2. Single-particle spectrum of D1 (104 Å × 26 Å), D2 (142 Å × 36 Å), and D3 (156 Å × 39 Å). $e1$, $e2$, $e3$, $e4$ are the InAs-confined electron states, while h1, h2, h3, and h4 are the interface localized hole states.

exchange potential has a long-range component [21], we do allow its screening.

Single-particle states.—Diagonalization of the atomistic single-particle pseudopotential Hamiltonian gives the confined single-particle electron and hole energy levels shown in Fig. 2. The corresponding wave functions for D2 are shown in Fig. 3. We see that the four InAs-confined electron states $e1$, $e2$, $e3$, $e4$ move *down* in energy as the dot size increases, whereas the interfacially confined (see. Figure 3) hole states h1 and h2 move *up* in energy as the size increases. For the smallest dot D1, there is a finite, single-particle gap of 96 meV between the first confined electron and hole states. For dot D2, the gap reduces to ~6 meV. For the large dot D3, the lowest InAs-confined electron level lies *below* the VBM of the InSb barrier and hybridizes with it. The single-particle gap is thus negative, signaling a charge transfer from InSb to InAs.

Many-body states.—The energies were carefully converged by increasing the basis in the many-body expansion. We construct all Slater determinants possible from the six lowest energy holes and all confined electron states (there are only two bound electron states in D1 and four in D2). For a single exciton in D2, this gives 96 CI basis determinants, whereas for the biexciton this gives 1848 CI determinants. For an uncorrelated electron-hole pair, the total energy is E_g, whereas correlation could reduce the energy of the monoexciton E_X by $\Delta_X \equiv E_g - E_X$. Biexcitons E_{XX} could be bound with respect to two excitons by $\Delta_{XX} \equiv 2E_X - E_{XX}$. The CI energies are shown in Fig. 4. The results show that, for dot D1, $E_X = 79$ meV and $E_{XX} = 161$ meV both positive, i.e, correlation energies do not overcome the single-particle gap. However, for dot D2 we find that correlation reduces the total energy of the single electron-hole pair from $E_g = +6$ meV to $E_X = -9$ meV. A negative total energy $E_X < 0$ means that the exciton can form spontaneously. For two electron-hole pairs, the reduction is from $2E_g = +12$ meV to $E_{XX} = -15$ meV. Thus, the energy to add a second exciton is $E_{XX} - E_X = -6$ meV per dot. For three electron-hole pairs, the total energy is $E_{XXX} = +90$ meV per dot, and the addition energy is 105 meV. Comparing the various total energies, we see that two electron-hole pairs represent the ground state. The next question is whether the two electron-two hole state form a bound biexciton or not. We find that $\Delta_{XX} = -3$ meV, showing that the 4-particle state is not a bound biexciton, but two excitons confined to the dot.

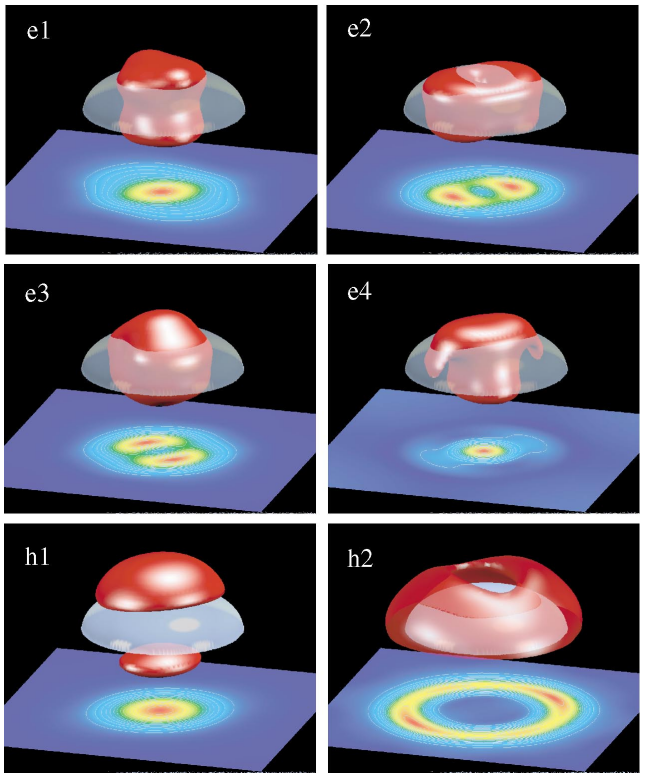

FIG. 3 (color). Wave functions of the InAs-confined electron states ($e1$–$e4$) and the first two hole states (h1–h2). The transparent lenses indicate the positions of the InAs dots. The isosurfaces enclose 50% of the state density except for $e4$, which is only weakly confined. For $e4$, the isosurface enclose only about 10% of the state density. The contour plot are slices of the density taken from chosen planes.

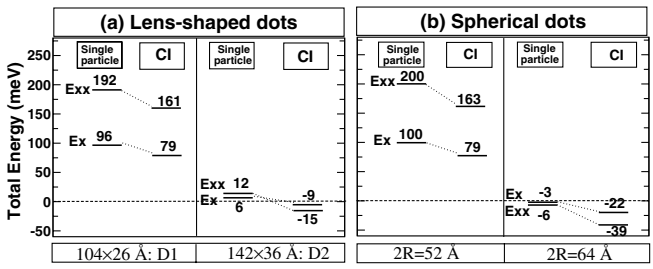

FIG. 4. Exciton and biexciton energies of (a) lens-shaped and (b) spherical InAs dots embedded in the InSb matrix.

To see whether the shape of the dot affects these conclusions, we performed similar calculations for spherical InAs/InSb QDs. The critical diameter for the single-particle band gap closure is now around $2R = 64$ Å. The calculated exciton and biexciton energies are shown in Fig. 4(b) for two diameters (52 and 64 Å). For the $2R = 64$ Å dot, we find an exciton energy of $E_X = -22$ meV, and a biexciton energy of $E_{XX} = -39$ meV. Again the two electron-hole-pair state is the ground state and we have $\Delta_X = 19$ meV and $\Delta_{XX} = -5$ meV. The biexciton is also unbound.

Properties of excitonic ground state.—The two electron-hole-pair ground state is similar to a helium atom in the sense that there are two positive and two negative Coulomb bound charges. These states can be identified as ''excitonic molecule'' states [4]. The calculated permanent electric dipole moment $\mathbf{p} = \int \mathbf{x}\rho(\mathbf{x})d^3x$ for the exciton and biexciton of the lens-shaped dot D2 are aligned along [001] direction (growth direction), and amount to $p_z = 3.58e$ Å for the exciton and $p_z = 7.16e$ Å for the biexciton. These dipoles could be measured experimentally and since the exciton binding energy is so high ($\Delta_X \sim 15$ meV), it can be studied at rather high temperatures.

Recent developments in epitaxial growth made it now possible to grow arrays of QDs [23]. Given these excitonic dipoles, it is interesting to study the collective behavior of excitons in the QD arrays due to dipolar interactions. At a *low dot density*, where the QDs are far apart, the excitons behave like in the single dot and couple only weakly via dipole-dipole interactions. This is the classic problem of Bose-Einstein condensation (BEC) in dipolar Bose gases, which is currently attracting a lot of attention [24,25]. The BEC of dipolar gases may have various phases depending on details of the interactions [26]. Since excitons have lighter masses and stronger dipole-dipole interactions than atoms, they are therefore ideal candidates for the study of the different BEC phases. In the case of dot arrays, the exciton energy in a single dot $E_x < 0$ signals only the instability towards the excitonic insulator, where it must be renormalized by the dot-dot interactions. Furthermore, the size distribution and disorder of the QD lattice may lead to a more complicated ''Bose glass'' phase [27,28]. Thus, the excitonic ground states in dot arrays bring up challenging and interesting problems to both theorists and experimentalists. A full treatment of the various phases is out of the scope of the current letter and is a good subject for further studying.

At *medium and high* densities, where the QDs have stronger coupling, there could be numerous phases as a function of carrier density and mass ratios, as proposed in Ref. [4]. In these regions, the picture of (bi)exciton on a single QD is not valid anymore. However, the electron-hole density and mass ratio can be tuned via the parameters of the dot arrays, such as the size and confining potential of a single dot, the density of dots, and even the structure of the dot arrays, thus make them very promising for the study of the electron-hole phase diagram.

To conclude, our pseudopotential many-body calculations predict a valence-to-conduction single-particle energy level crossover and the spontaneous formation of a biexcitoniclike ground state at a critical size for lens-shaped and spherical InAs/InSb dots. Two reasons make this type III QD system a very promising candidate to study excitonic ground states. First, the electron-hole energy gap is tunable by the QDs size alone, and second, the excitons have much larger binding energies than in the bulk, or in quantum wells due to the confinement of both electrons and holes in all dimensions. Experimental studies are called for on such a proposed excitonic ground state.

This work was supported by U. S. DOE-SC-BES-DMS, under LAB 3-17 initiative Grant No. DEAC36-98-GO10337.

[1] N. F. Mott, Philos. Mag. **6**, 287 (1961).
[2] L. V. Keldysh and Y. V. Kopaev, Fiz. Tverd. Tela (Leningrad) **6**, 2791 (1964) [Sov. Phys. Solid State **6**, 2219 (1965)]; L. V. Keldysh and A. N. Kozlov, Zh. Eksp. Teor. Fiz. **54**, 978 (1968) [Sov. Phys. JETP **27**, 521 (1968)].
[3] B. I. Halperin and T. M. Rice, Rev. Mod. Phys. **40**, 755 (1968).
[4] P. B. Littlewood *et al.*, Phys. Status Solidi B **234**, 36 (2002).
[5] *Bose-Einstein Condensation*, edited by A. Griffin *et al.* (Cambridge University Press, Cambridge, England, 1995).
[6] L. V. Butov *et al.*, Nature (London) **417**, 47 (2002).
[7] B. Bucher *et al.*, Phys. Rev. Lett. **67**, 2717 (1991).
[8] S. Datta *et al.*, Phys. Rev. B **32**, 2607 (1985).
[9] X. Zhu *et al.*, Phys. Rev. Lett. **74**, 1633 (1995).
[10] R. Magri *et al.*, Phys. Rev. B **61**, 10 235 (2000).
[11] J. P. Cheng *et al.*, Phys. Rev. Lett. **74**, 450 (1995).
[12] D. Bimberg *et al.*, *Quantum Dot Heterostructures* (John Wiley & Sons, New York, 1999).
[13] R. Magri and A. Zunger, Phys. Rev. B **65**, 165302 (2002); R. Magri *et al.* (unpublished).
[14] A. Zunger, Phys. Status Solidi B **224**, 727 (2001).
[15] *Landolt-Börnstein*, edited by O. Madelung (Springer-Verlag, Berlin, 1987), Vol. 22a.
[16] M. Pinczolits *et al.*, Appl. Phys. Lett. **73**, 250 (1998).
[17] P. N. Keating, Phys. Rev. **145**, 637 (1966).
[18] G. E. Pikus and G. L. Bir, Phys. Rev. Lett. **6**, 103 (1961).
[19] L.-W. Wang and A. Zunger, Phys. Rev. B **59**, 15 806 (1999).
[20] G. Bester *et al.*, Phys. Rev. B **67**, 161306 (2003).
[21] A. Franceschetti *et al.*, Phys. Rev. B **60**, 1819 (1999).
[22] G. Onida *et al.*, Rev. Mod. Phys. **74**, 601 (2002).
[23] Q. Xie *et al.*, Phys. Rev. Lett. **75**, 2542 (1995).
[24] F. Dalfovo *et al.*, Rev. Mod. Phys. **71**, 463 (1999).
[25] L. Santos *et al.*, Phys. Rev. Lett. **85**, 1791 (2000).
[26] K. Góral *et al.*, Phys. Rev. Lett. **88**, 170406 (2002).
[27] J. A. Hertz *et al.*, Phys. Rev. Lett. **43**, 942 (1979).
[28] M. P. Fisher *et al.*, Phys. Rev. B **40**, 546 (1989).